PHYSICAL REVIEW B

CONDENSED MATTER

THIRD SERIES, VOLUME 44, NUMBER 5 1 AUGUST 1991-I

Calculation of the $F_{H2}(OH^-)$-center absorption bands in CsCl

Philip W. Gash

Department of Physics, California State University, Chico, Chico, California 95929-0202

(Received 10 December 1990)

The $F_{H2}(OH^-)$-center electron-energy levels in CsCl are calculated with use of a pseudopotential formalism in which the model potential incorporates the point-ion potential, ion-size effects, and the interaction with both the OH^- permanent and displacement dipole moments. Electronic polarization and a radial A_{1g} distortion of the nearest-neighbor cations are treated as perturbations. The $F_{H2}(OH^-)$-center model is an F center between two NNN OH^- ions along $\langle 001 \rangle$ with the permanent dipoles pointing toward the vacancy, and the configuration has D_{4h} point-group symmetry. The OH^- displacement from the lattice site along $\langle 001 \rangle$ is taken as a model parameter, and it is adjusted to obtain agreement with the absorption bands. The model yields an average $F_{H2}(2)$-band peak at 2.25 eV, compared with the observed value of 2.33 eV, and an $F_{H2}(1)$-band peak at 1.38 eV, compared with the observed value of 1.31 eV. The optimum OH^- displacement is 0.43 Å toward the vacancy accompanied by an 8% outward A_{1g} radial displacement of the NN Cs^+ ions. The caluclated A_{1g} localized-mode frequency is 2.42×10^{12} Hz. The calculated ratio of the band oscillator strengths is 4.2, which is in good agreement with the experimental value of 3.2.

I. INTRODUCTION

F centers associated with the defect molecular ions CN^- and OH^- in the Cs halides have been studied recently because of their special optical properties attributed to the interaction between the F-center electron and molecular ion.[1-7] These defect complexes, the $F_H(CN^-)$ and $F_H(OH^-)$ centers, exhibit two absorption bands with splittings of 0.27 and 0.74 eV, respectively. For both centers the high-energy absorption band, the $F_H(2)$ band, shows spin-orbit splitting; it is 0.05 eV for the $F_H(OH^-)$ center in CsCl.[6] The point-group symmetry of the F_H center is C_{4v}, with the molecular axis along $\langle 001 \rangle$, and the ion is located at the next-nearest-neighbor (NNN) position to the vacancy. A model calculation of the absorption bands for both centers requires the molecular ion's center of mass to be slightly displaced from the lattice site toward the vacancy along the $\langle 001 \rangle$ direction and requires the ion's intrinsic electric dipole moment to point toward the F-center vacancy.[3,4] The $F_H(OH^-)$-center electron ground and excited states, $|1A_1\rangle$, $|2A_1\rangle$, and $|2E\rangle$, respectively, are linear combinations of the $|S\rangle$ and $|P\rangle$ basis states of the F-center electron, where the mixing is produced by the electric fields from both the OH^- ion's permanent and displacement electric dipoles.

Recently, an additional center—the $F_{H2}(OH^-)$ center—has been found to exhibit a significantly increased splitting of the two absorption bands: 1.02 eV in CsCl and 0.99 eV in CsBr.[6] The center is produced only in samples with high OH^- concentrations by repeated aggregation and bleaching of the $F_H(OH^-)$ centers in the F and $F_H(2)$ bands at 180 K. They cannot be produced in samples with low OH^- concentrations. These properties are similar to those of F_B(Na) centers in KCl, where bleaching in the F_A(Na) band produces an F center between two Na^+ ions only in higher-concentration samples.[8]

In CsCl the $F_{H2}(OH^-)$ center's high band—the $F_{H2}(2)$ band—is split with peaks at 2.36 and 2.30 eV, and the low band—the $F_{H2}(1)$ band—is centered at 1.31 eV. In comparison with the $F_H(OH^-)$ absorption bands, the major difference is that the low-energy band is shifted 0.27 eV downward from 1.58 to 1.31 eV, see Table I. The oscillator strength ratio $f(F_{H2}(2)/f(F_{H2}(1))$ is 3.2, which suggests a 2:1 ratio in the transition-matrix elements.[9,10] The bands are polarized with respect to the $\langle 001 \rangle$ axis of the $F_H(OH^-)$ center, with the $F_{H2}(2)$ band perpendicular and the $F_{H2}(1)$ band parallel to the axis. Magnetic circular dichroism measurements yield two negative spin-orbit coupling parameters (one parallel and one perpendicular), which is indicative of a one-electron center in a tetragonal environment.[10] Irradiation in the $F_{H2}(2)$ band with $\langle 001 \rangle$ polarized light produces a $\langle 001 \rangle$ linear dichroism

TABLE I. Peak energies of the absorption bands for the F, $F_H(OH^-)$, and $F_{H2}(OH^-)$ centers in CsCl. Values are in eV and are taken from Ref. 33.

F	$F_H(2)$	$F_H(1)$	$F_{H2}(2)$	$F_{H2}(1)$
2.14	2.31	1.58	2.33	1.31

of opposite signs for the two bands, and irradiation with ⟨110⟩ light shows no linear dichroism.

Based on these properties, the following $F_{H2}(OH^-)$ model is adopted: An F center is located between two OH^- ions located at NNN sites along the ⟨001⟩ axis, as shown in Fig. 1. The rationale for two OH^- ions is twofold: (1) The centers are not produced in samples with low OH^- concentrations, where the probability of dual proximity is small. (2) The reduced value of spin-orbit coupling parameter compared to that of the $F_H(OH^-)$ center is indicative of an extra perturbation, such as another OH^- ion.[10] One additional model feature is that the OH^- electric dipoles are oriented toward the F-center vacancy in order to account for the wide splitting of the bands. A dipole moment oriented outward pushes the bands together;[3] hence, an additional OH^- dipole pointing inward pushes the bands farther apart. With both dipoles pointing inward, the point-group symmetry of the center is D_{4h}.

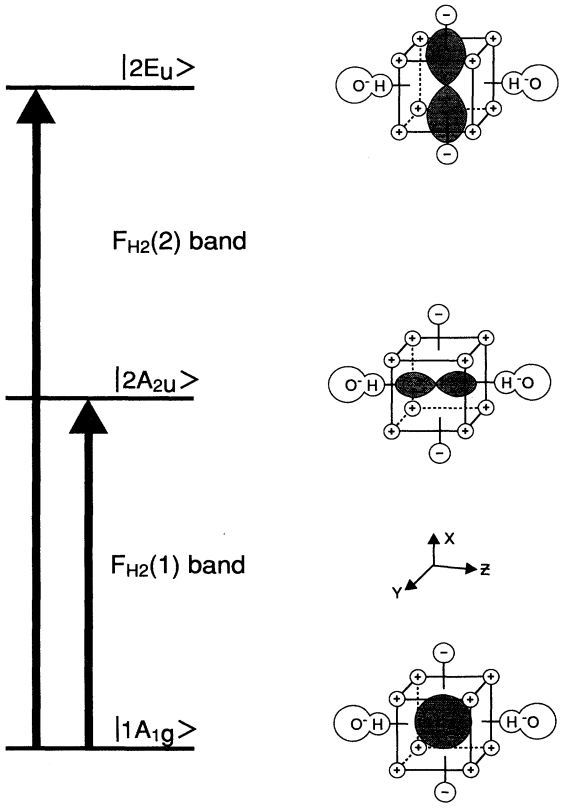

FIG. 1. Schematic diagram of the $F_{H2}(OH^-)$ center in CsCl showing location and orientation of the OH^- ions, the angular configuration of the states, and the transitions producing the $F_{H2}(2)$ and $F_{H2}(1)$ bands.

The purpose of this paper is to account for the energies and symmetry properties of the $F_{H2}(2)$ and $F_{H2}(1)$ absorption bands with a model calculation that incorporates the point-ion potential, ion-size effects, the OH^- permanent electric dipole moment, the OH^- center-of-mass displacement, electronic polarization, and nearest-neighbor (NN) distortion.

II. MODEL CALCULATION

A. Bartram-Stoneham-Gash pseudopotential method

Bartram, Stoneham, and Gash (BSG) derived a defect-electron pseudopotential that provides a tractable means of performing a variational calculation for the F-center electron which takes into account ion-size effects: the electrostatic and exchange interactions, and the orthogonalization to the ion-core states.[11] The F bands in the rocksalt-structure alkali halides are calculated using the pseudopotential, and they are in good agreement with the observed values. The pseudopotential is expressed by

$$V_p = V + P(V^* - V) , \tag{1}$$

where P is a projection operator made up of the ion-core states, V is the electric potential, and V^* is the expectation value of V_p computed using the normalized trial F-center pseudo-wave-function $|\Phi\rangle$. In ionic solids the tight-binding model is adopted so that P is made up only of free-ion wave-functions, and the free-ion wave function overlap between neighboring ions is neglected; in addition, the variation of the trial function over the ion cores is neglected. Physically, these conditions mean that inside the ions the F-center wave-function oscillations are orthogonal to the ion-core states, and outside the ions, the wave function is equal to the pseudo-wave-function $|\Phi\rangle$. With these restrictions the expectation value of V_p—the potential energy of the F-center electron—is given by

$$\langle\Phi|V_p|\Phi\rangle = \langle\Phi|V_{\rm PI}|\Phi\rangle + \sum_\gamma C_\gamma |\Phi(\mathbf{R}_\gamma)|^2 , \tag{2}$$

where the first right-hand term is the expectation of the point-ion potential, and in the second term, the summation is over all ions, each located at position $\mathbf{R}_\gamma$. The second term incorporates the ion-size effects. The coefficient C_γ is given by

$$C_\gamma = A_\gamma + (V^* - U_\gamma)B_\gamma . \tag{3}$$

The A_γ and B_γ coefficients are ion dependent, and they have been calculated by BSG for several mono- and divalent ions.[11] The U_γ term represents the potential at each ion site γ due to all other changes, including the OH^- ion's permanent and displacement dipoles.

The eigenvalue computational procedure requires iteration to self-consistency, which is accomplished in the following fashion: A trial pseudo-wave-function varia-

tional parameter value is selected, and the expectation value of the point-ion potential is computed for a starting value of V^*; then the expectation value of the pseudopotential is calculated; the new value of V^* is used to recompute the expectation value; and the process is repeated until V^* converges, typically to 1 part in 10^5 after ten iterations. The parameter value is changed and the process is repeated until the minimum-energy eigenvalue is found.

B. F_{H2} (OH^-)-center pseudopotential

In the present case, the potential from the finite-size OH^- permanent electric dipole and the displacement electric dipole are included in V together with the ion-size effects. The pseudopotential for the $F_{H2}(OH^-)$-center electron is given by

$$V_p = V_{\rm PI} + V_\alpha + V_\beta + \sum_\gamma C_\gamma \delta(\mathbf{r} - \mathbf{R}_\gamma) , \quad (4)$$

here V_α is the parameter electric dipole potential, V_β is the displacement dipole potential, and $\mathbf{r}$ is a general point.

C. OH^- finite-size electric dipole potential

In Eq. (4) the potentials U_γ and V_α require knowledge of the point charges and separation used to model the OH^- permanent electric dipole moment. The moment has been the subject of several experimental and theoretical studies.[12–18] Two theoretical studies include calculations of the permanent electric dipole moment: One is a self-consistent calculation and the other uses an electron-gas model, in which the exchange interaction is approximated by an electron-density term. The electron-gas model yields wave functions which do not decrease as rapidly at large distances as the self-consistent wave functions.[19,20] The dipole expectation value is very sensitive to the wave-function behavior in the outer regions because the radial integrand puts more weight on the larger radial values; hence the electron-gas model wave functions produce larger dipole moment expectation values. For this reason, the smaller of the two calculated moments is taken to be more representative of the OH^- permanent electric dipole moment. In this work we use the dipole moment of Cade[12] and model it as two equal and opposite charges of 2.06×10^{-10} esu separated by the OH^- bond length of 0.95 Å. The experimentally determined values of the electric dipole moment are not considered because they may include the dipole moment due to a center-of-mass displacement. There are two dipole configurations consistent with D_{4h} symmetry: Both dipoles point either into or away from the vacancy along $\langle 001 \rangle$. The inward configuration was selected as it produces the larger band splitting.

D. OH^- displacement dipole moment

In the rocksalt-structure alkali halides, a center-of-mass displacement of the OH^- ion from the lattice site by 0.2–0.3 Å is necessary to obtain agreement with the observed librational frequencies and splitting from tunneling;[21] hence a realistic model for OH^--ion behavior must allow for center-of-mass displacement. Equal displacements of the two OH^- ions toward or away from the vacancy are consistent with the D_{4h} symmetry. The OH^- displacement is modeled by placing a positive point charge at the lattice site to neutralize the negative charge and then placing a negative point charge on the center of mass along $\langle 001 \rangle$. This is equivalent to locating a dipole moment—the displacement dipole—along $\langle 001 \rangle$ and pointing from the center-of-mass position to the lattice site. Using the displacements above, the displacement dipole moment is on order of 1.0×10^{-18} esu cm. It is about one-half of the permanent dipole, and with two dipoles present, we expect them to make significant contributions to the F-center electron's energy.

E. $F_{H2}(OH^-)$-center electron basis states

The angular dependence of the defect-electron basis states must transform as the irreducible representations of D_{4h}. The basis states, unperturbed by the electric dipoles, are the $|S\rangle$ and three $|P\rangle$ states. Inspection of the character table shows that the $|S\rangle$ state transforms as the A_{1g} representation, the $|Z\rangle$ state transforms as A_{2u}, and the $|X\rangle$ and $|Y\rangle$ states transform as E_u. Therefore, there will be no mixing of the basis states by diagonalizing the Hamiltonian. This property contrasts with that of the $F_H(OH^-)$ center where the single dipole's electric field strongly mixes the $|S\rangle$ and $|Z\rangle$ states in the ground and lower excited states.[4] The inversion element of D_{4h} precludes the existence of an electric field at the vacancy center; hence there is no mixing of the basis states. To be consistent with atomic spectroscopic notation, the ground state is denoted by $|1A_{1g}\rangle$, and the two excited states are denoted by $|2A_{2u}\rangle$ and $|2E_u\rangle$

F. Dipole potential matrix elements $\langle V_\alpha \rangle$ and $\langle V_\beta \rangle$

The evaluation of the dipole potential matrix elements is simplified by expanding the potential from each dipole charge in an infinite series of products of spherical harmonics and radial functions centered on the vacancy.[22] The first three expansion terms of the potential $Vq(\mathbf{r})$ at a position $\mathbf{r}$ due to a single charge q located at a distance R along the z axis are given by

$$Vq(\mathbf{r}) = Y_{00}C_{00}(1/R) + Y_{10}C_{10}(r/R^2) = Y_{20}C_{20}(r^2/R^3) ,$$

for $r < R$, and

$$Vq(\mathbf{r}) = Y_{00}C_{00}(1/r) + Y_{10}C_{10}(R/r^2) + Y_{20}C_{20}(R^2/r^3) ,$$

for $r > R$, and with $C_{00} = q\sqrt{4\pi}$, $C_{10} = q\sqrt{4\pi/3}$, and $C_{20} = q\sqrt{4\pi/5}$. The arguments of the spherical harmonics $Y_{\rm LM}$ are the angular coordinates of the position vector $\mathbf{r}$.

The expansion must have D_{4h} symmetry; therefore, the only nonzero terms which contribute to the matrix elements are those which transform as the spherical harmonics Y_{00} and Y_{20}.[23] Additional higher-order terms are

present, but they are of no physical interest because they do not couple the basis states. We denote these two terms for the permanent electric dipole potential by $V_{\alpha 0}$ and $V_{\alpha 2}$, and for the displacement dipole by $V_{\beta 0}$ and $V_{\beta 2}$. Physically, the expectation value $\langle V_{\alpha 0} \rangle$ represents the average dipole potential at the vacancy center, and the expectation value $\langle V_{\alpha 2} \rangle$ is a measure of the dipole's electric-field gradient averaged over the vacancy.

G. Polarization correction

The electric polarization contributes to the defect-electron energy because of the large polarizability of the NN Cs^+ ions. The interaction between the electronic point dipoles induced on the ions and the defect electron is taken into account using the method originated by Gourary and Adrian.[24] The expression for the decrease in defect-electron energy is given by

$$-\sum_s N_s \alpha_s Q_s^2 / R_s^4 , \tag{5}$$

where R_s is the shell radius, α_s is the electronic polarizability,[25] N_s is the number of ions on shell s, and Q_s is the spherically averaged net charge between the vacancy and the shell s. The net charge produces an electric field at each ion site, and it induces a point dipole on the ion. The net charge consists of the positive charge necessary to replicate the vacancy, plus that portion of the defect-electron charge out to R_s; hence the greater the localization of the defect electron, the smaller the polarization contribution. The series converges rapidly, and it is carried out to only ten shells.

H. Distortion correction

It is recognized that the static displacements of the NN ions from the lattice sites can be written as linear combinations of distortions, each labeled by the irreducible representations of D_{4h}. To the extent that the static displacements are linear in each distortion, only that labeled by A_{1g}, will contribute to a shift in the electronic ground-state energy, and it also contributes shifts in all other electronic states. Distortions transforming as the other irreducible representations of D_{4h} selectively split and shift the excited states. We assume that the totally symmetric distortion has the lowest energy and is therefore the major component of the NN static displacements; accordingly, in the model, the eight Cs^+ ions nearest to the vacancy are allowed to undergo a radial A_{1g} distortion with the remaining ions fixed at the lattice sites.

The distortion contribution to the defect-electron energy is treated as a perturbation, and it is determined using the method developed by Gourary and Adrian,[24] which is outlined briefly here: First, the ground-state defect-electron trial wave function $|1A_{1g}\rangle$ is determined, which minimizes the energy eigenvalue, as discussed in Sec. II A. Next, a radial displacement is selected; then the changes in the point-ion energy and the ion-size effect energy are determined, together with the lattice energy.

The lattice energy is made up of the electrostatic energy of the NN cations interacting only with their NN anions, a repulsive overlap term which uses an exponent value of 9 in the potential,[26] and the potential energy of the cations in the presence of the OH^- permanent and displacement dipoles. The sum of the energy changes plus the lattice energy is referred to as the electron-lattice energy.

The electron-lattice energy is computed for several radial displacements until a minimum is found, and that displacement is taken as the equilibrium lattice distortion. The electron-lattice energy is added to the ground-state energy eigenvalue and the polarization correction to form the system energy. It represents the ground-state energy of the defect electron and lattice system. Within the constraints of the Born-Oppenheimer approximation, the system energy is the major portion of the harmonic potential for nuclear motion. The computation is repeated using the excited-state wave functions and the equilibrium lattice distortion, since the absorption process is a vertical transition.[27] The difference in the system energy values is equal to the absorption band energy.

I. Selection of α for CsCl

BSG found it necessary to reduce the relative contributions of A_γ compared to B_γ by a factor α, because A_γ produces a potential that is too repulsive for large cations and too attractive for large anions. Some adjustment is expected because of the use of free-ion wave functions, the neglect of overlap, and the neglect of the trial function variation over the ion cores. They find that an α value of 0.53 gives the best least-squares fit to the F bands in the rocksalt-structure alkali halides. Subsequent investigations show that α is both ion and defect dependent; hence we expect that BSG's value is not appropriate for $F_{H2}(OH^-)$ centers in the Cs halides.[28–30] The BSG pseudopotential is used to calculate the F-band energy in CsCl, with $\alpha = 0.53$, and the energy is too low. The value of α is varied to obtain agreement with the observed 2.15-eV F-band energy, where the point-ion potential, the ion-size effects, electronic polarization, and NN distortion are taken into account. The value which gives agreement with the F-band energy is $\alpha = 0.74$, and it is used in the $F_{H2}(OH)^-$-center calculations.

J. A_γ and B_γ coefficients for OH^-

The analysis requires the values of A_γ and B_γ, and they have not been calculated using the OH^- electronic wave functions. Nonetheless, there is reasonable justification to approximate the coefficients using the O—H bond length. BSG presented simple arguments which show that A_γ is proportional to the ionic area and that B_γ is proportional to the ionic volume. When the coefficient values are plotted versus the ionic area and ionic volume using the accepted ionic radii,[25] the curves are linear; therefore, the coefficients for OH^- are approximated using a least-squares fit with 0.95-Å bond length for the ionic radius.

K. Trial pseudo-wave-functions

The basis states are products of a radial function and a spherical harmonic function, as previously discussed in Sec. II E. Two trial radial functions are used; the one for the ground state with $|S\rangle$ angular dependence is given by

$$J_0(x)\exp(-x^2) , \tag{6}$$

where $x=\beta r/a$ with the variational parameter β, and internuclear separation $a=3.56$ Å. The radial function used for the $|P\rangle$ excited states is the Gourary and Adrian type-II function[24] given by

$$J_1(x)\exp(-\epsilon) , \tag{7}$$

when $r<a$, and where $x=\mu r/a$, with the following relationship between μ and ϵ:

$$\epsilon=3-\mu^2/[1-\mu\cot(\mu)] . \tag{8}$$

When $r>a$, the function has the form

$$J_1(\mu)(r/a)\exp(-\epsilon r/a) . \tag{9}$$

In the expressions above, the normalization constant is suppressed for clarity, and $J_n(x)$ denotes a spherical Bessel function of order n.

In the expectation values, the radial integrals are evaluated using a Newton-Cotes five-point quadrature for 320 points from the vacancy center to the 86th shell.[31] The expectation value of the kinetic energy is calculated using Löwden's simplified expression.[32] The first-order derivatives are evaluated using a five-point scheme.[33]

III. CALCULATION OF THE $F_{H2}(OH^-)$-CENTER ABSORPTION BANDS

A. $F_{H2}(OH^-)$-center energy levels

The $F_{H2}(OH^-)$ center exhibits two absorption bands, the $F_{H2}(1)$ band that is centered at the low energy of 1.31 eV and the $F_{H2}(2)$ band that is peaked at 2.36 and 2.30 eV as a result of the spin-orbit interaction, see Table II. In this calculation the spin-orbit interaction is neglected because the objective is to explain and understand the physical origin of the large 1.02-eV splitting between the two bands.[34]

We let the OH^- ions reside on the $\langle 001\rangle$ axis at the two NNN positions where they substitute for Cl^- ions, and the dipole moments point toward the vacancy. The basis pseudo-wave-functions are discussed in Secs. II E and II K. Since they transform as individual irreducible representations of D_{4h} symmetry, the energy eigenvalues are obtained by simply calculating only the expectation values of the Hamiltonian. After the energy eigenvalues and variational parameters are determined, the polarization contribution is calculated using the technique discussed in Sec. II G. The procedure is repeated for two other values of the variational parameter and then a parabolic curve is passed through the energy values. The value of the variational parameter corresponding to a minimum energy is determined. The energy eigenvalues and polarization contribution are recomputed for that value of the parameter, and they are taken as the optimum values. The next step is to select a A_{1g} radial displacement, as discussed in Sec. II H, and calculate the corresponding electron-lattice energy. From these values the system energy is determined. The energy values are presented in Table III.

Figure 2 displays the system energy curves for the three electronic states and illustrates the transitions for both absorption bands. The ground-state curve has a minimum at 8% outward radial displacement. Within the context of the Born-Oppenheimer approximation, the curves form the major portion of the harmonic potential for the nuclear motion.[35] A least-squares parabolic fit of the curve yields a A_{1g} local-mode frequency of 2.42×10^{12} Hz (80.6 cm^{-1}) for the NN Cs^+ ions. For purposes of comparison, the peak of the CsCl phonon spectrum is 4.77×10^{12} Hz at the Γ point in the zone.[36]

Section II D discusses the reasons for expecting that the OH^- ions' center of mass may be displaced from the lattice site. This feature is incorporated into this model in the following manner: For a given displacement, the system energy for each state is computed using the technique discussed above. The transition energies as a func-

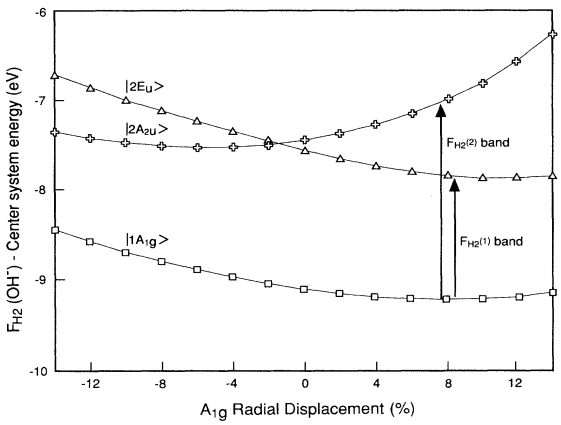

FIG. 2. System energy for all three states of the $F_{H2}(OH^-)$ center is shown as a function of the radial displacement of the NN Cs^+ ions; the units are a percentage of the internuclear separation. The optimum outward displacement of 8% corresponds to the minimum in the grounds-state $|1A_{1g}\rangle$ curve. The transitions to the excited states responsible for the $F_{H2}(2)$ and $F_{H2}(1)$ bands are slightly displaced for purposes of illustration.

TABLE II. Comparison of observed and calculated absorption band energies of the $F_{H2}(OH^-)$ center in CsCl at 13 K. All energies are in eV.

Band	Observed	Calculated
$F_{H2}(1)$	1.31	1.38
Average $F_{H2}(2)$	2.33	2.25

TABLE III. Contributions to the electron-energy levels when the two OH^- dipoles point toward the vacancy, each center of mass is displaced 0.43 Å toward the vacancy, and the NN cations are displaced radially outward 8%. All energies are in eV.

State parameter	Energy eigenvalue	Pol.	Electron-lattice energy	System energy
$\|1A_{1g}\rangle$ $\beta=1.137$	−6.81	−0.06	−2.28	−9.15
$\|2A_{2u}\rangle$ $\mu=3.762$	−5.27	−0.06	−2.44	−7.77
$\|2E_u\rangle$ $\mu=3.404$	−4.93	−0.29	−1.68	−6.90

tion of displacement are computed, and that displacement value is taken as optimum for which both transition energies agree with experimental values.

B. Oscillator strength ratios

The oscillator strength or integrated intensity for a transition from electronic state $|i\rangle$ to state $|j\rangle$ with the electric-field polarization along $\mathbf{r}$ is proportional to the product

$$\delta E|\langle i|\mathbf{r}|j\rangle|^2 , \tag{10}$$

where δE is the peak energy, and $\mathbf{r}$ is the F-center electron position coordinate, such as x, y, or z. It provides a very sensitive measure of the wave functions because the factor $\mathbf{r}$ places greater weight on the extremities of the wave function. The energy-level calculation is performed using a trial pseudo-wave-function $|\Phi\rangle$; hence, within this scheme, the oscillator strength expression above must be rewritten in terms of it. The relationship between the F-center electron wave function $|i\rangle$ and $|\Phi\rangle$ is given by $|i\rangle=N_i(1-P)|\Phi(i)\rangle$, where N_i is a normalization constant, and P is a projection operator containing all the electron-core states. In the pseudopotential method formalism, the free-ion-core states are used in P; their overlap between neighboring lattice sites is neglected, as well as the variation of the pseudo-wave-function $|\Phi\rangle$ over the ion cores. Within this context Eq. (10) is rewritten as

$$\delta E\, N_i N_j \left|\langle\Phi(i)r\Phi(j)\rangle - \sum_\gamma B_\gamma[\Phi^*(i)]_\gamma r_\gamma[\Phi(j)]_\gamma\right|^2 , \tag{11}$$

where the summation is over the ion states γ, B_γ is the coefficient discussed in Sec. II J, $[\Phi(j)]_\gamma$ is the pseudo-wave-function corresponding to the electron state j, evaluated at the lattice site γ, and r_γ is the x, y, or z coordinate from the vacancy to site γ.

The calculated and experimental oscillator strength ratios are shown in Table IV. The ratio is calculated summing over 15 shells; as a practical matter, it converged to better than 95% of its final value after the first four shells. The nonorthogonalized ratio is calculated using only the first term in Eq. (10), whereas the orthogonalized ratio is calculated using both terms. The physical difference between the two ratios is the degree to which the extremities of the wave functions are taken into account. In the vacancy the pseudo-wave-function is the wave function, but in the region of the ions, the pseudo-wave-function is orthogonal to the core states.

The nonorthogonalized ratio of 3.7 for the $F_{H2}(OH^-)$ center is in good agreement with the experimental ratio of 3.2. The agreement is indicative of the contribution due to the wave function inside the vacancy. The orthogonalized ratio of 4.2 is shifted clearly opposite to what is expected. The larger ratio is due to either the summation contribution being too large for the $|2E_u\rangle$ state or too small for the $|2A_{2u}\rangle$ state. In either case the origin is twofold: First, the summation places greater weight on the outer regions of the pseudo-wave-function, and second, the B_γ term only includes contributions from the ion-core $|S\rangle$ states, and so the pseudo-wave-function is not fully orthogonalized to all the ion-core states. The value 4.2 is produced by a matrix-element ratio $\langle 1A_{1g}|x|2E_u\rangle/\langle 1A_{1g}|z|2A_{2u}\rangle$, about 15% larger than that corresponding to the experimental value.

The oscillator strength ratio for the $F_H(OH^-)$ bands are included for purposes of comparison and because the $F_H(OH^-)$ energy levels are discussed in Sec. III C. Using the orthogonalized functions, the ratio is 33.7, which is too large. This value is produced by a matrix-element ratio $\langle 1A_1|x|2E\rangle/\langle 1A_1|z|2A_1\rangle$, about 3.5 times larger than that corresponding to the experimental value. The $F_{H2}(2)$- and $F_H(2)$-band oscillator strengths are comparable, whereas the $F_H(1)$-band strength is substantially smaller than that for the $F_{H2}(1)$ band and is responsible for the large ratio.

The physical reason for the smaller value is the small overlap of the ground and first excited states within the vacancy. The ground state localizes the charge in the vacancy on the side toward the OH^-, while it is localized on the opposite side of the vacancy in the first excited state. The large ratio brings into question the extent of

TABLE IV. Oscillator strength ratios of the higher-energy band/lower-energy band for the $F_H(OH^-)$ and $F_{H2}(OH^-)$ centers in CsCl.

Center	Experimental[a]	Calculated Non-orth.	Calculated Orth.
$F_H(OH^-)$	2.5	24.9	33.7
$F_{H2}(OH^-)$	3.2	3.7	4.2

[a]Reference 37.

the $|S\rangle$ and $|Z\rangle$ basis-state mixing, but does not bring into question that the states are split by the dipole's electric field and electric-field gradient.

The $F_H(OH^-)$ model calculation is questioned[7] because of the large value of the oscillator strength ratio and the calculation's failure to include mixing of the $|2S\rangle$ and $|2P\rangle$ states by the dipole's electric field, where it is assumed the states are degenerate. An additional variational calculation using hydrogenic wave functions was performed to resolve the degeneracy issue; it minimized only the kinetic plus the point-ion potential energy. The optimum radial wave functions[26] are $\exp(-r/.83)$ for the $|1S\rangle$ state, $(2.325-r/1.29)\exp(-r/1.29)$ for the $|2S\rangle$ state, and $(r/.64)\exp(-r/.64)$ for the $|2P\rangle$ state. The normalization constants are suppressed for clarity, the distance units are in angstroms, and $|1S\rangle$ and $|2S\rangle$ states are explicitly orthogonalized. The energies are -5.08 eV for the $|1S\rangle$ state, -1.87 eV for the $|2S\rangle$ state, and -3.63 eV for the $|2P\rangle$ state. The diffuse nature of the $|2S\rangle$ state contributes to its higher energy with a smaller kinetic energy (0.79 eV) and a higher potential energy (-2.66 eV) than the other two states. Within this model the fact that $|2S\rangle$ state energy is 1.76 eV above the $|2P\rangle$ state implies, to a first approximation, that $|2S\rangle$ state mixing can be neglected. Additional computations show this to be the case. When the OH^- dipole moment and displacement dipole matrix elements are included in the energy minimization, so that the F-center states are linear combinations of the $|1S\rangle$, $|2S\rangle$, and $|2P\rangle$ states, the $|2S\rangle$ state's expansion coefficient in the ground and first excited states is about 0.03. Additional calculations using the pseudopotential method to orthogonalize the hydrogenic trial functions to the core states, produce energy eigenvalues which are higher and more widely separated; hence neglecting the $|2S\rangle$ and $|2P\rangle$ state mixing is justified.

The large oscillator strength ratio is attributed to the general features of the $F_H(OH^-)$-center model calculation: In particular, the NN cations are allowed to distort, and with the exception of the OH^- ion, the other ions are fixed. In addition, the ion-ion forces treat the OH^- ion as spherical. In a more refined model which allows distortion of more than the NN cations and which treats the OH^- ion as nonspherical, one expects the expansion coefficients and the pseudo-wave-function to change. For example, if the $|1S\rangle$ state contribution to the ground state changes from 0.80 to 0.90, the oscillator strength ratio is reduced from 33.7 to 8.0. An increased $|1S\rangle$ contribution also reduces the pseudo-wave-function in the outer regions, which further decreases the ratio. The simple point is that the oscillator strength ratio is a severe test of a wave function, and small changes in the wave function produce large changes in the ratio.

C. Results and Discussion

The optimum A_{1g} outward radial displacement of the NN cations is 8% of the internuclear separation with a 0.43-Å center-of-mass displacement for each OH^- ion toward the vacancy. The displacement is about 3 times that for the $F_H(OH^-)$ center, and it is about 50% larger than those in the rocksalt-structure alkali halides.[4,20] The corresponding calculated $F_{H2}(2)$-band average energy is 2.25 eV, compared to the average $F_{H2}(2)$-band peak of 2.33 eV, and the calculated $F_{H2}(1)$-band energy is 1.38 eV, compared to the observed value of 1.31 eV.

The primary objective of this paper is to account for the approximate 1.02-eV separation of the absorption bands, and it is best done by starting with the F-center energy levels. In the $F_H(OH^-)$ center, the degenerate F-center states $|X\rangle$, $|Y\rangle$, and $|Z\rangle$ are split by the electric field because of both the permanent and displacement dipole moments of the single OH^- ion in the NNN position. We take the field at the vacancy along $\langle 001\rangle$, and it splits the triply degenerate states into one doubly degenerate state ($|X\rangle$ and $|Y\rangle$) and a single $|Z\rangle$ state. The $|Z\rangle$ state energy is lowered significantly because the electron is confined to move along $\langle 001\rangle$ where the positive part of the OH^- ion is closest to the vacancy. The degenerate-state energy is lowered only slightly since the electron is confined to move in the x-y plane perpendicular to the field.[4]

The second electric-field effect is to mix the $|Z\rangle$ and $|S\rangle$ states (see Table V), and that produces a repulsion of their energy levels; hence the $F_H(OH^-)$-center ground-state energy is pushed below the F-center $|S\rangle$ state energy.[4] Consequently, the ground to degenerate-state transition produces the $F_H(2)$ band with an energy (2.31 eV) greater than the F-band energy (2.15 eV). The transition to the lower excited state produces the $F_H(1)$ band with an energy (1.58 eV) lower than the F-band energy, in large part because of the significant lowering of the $|Z\rangle$ state energy.

The $F_{H2}(OH^-)$ center is formed by one more OH^- ion added to the $F_H(OH^-)$ center in the NNN position on the other side of the vacancy, so that the complex has inversion symmetry. The additional OH^- ion's first effect is to shift all the energy levels to lower values. Table VI shows the net OH^- dipole potential and electric-field gra-

TABLE V. Basis states and expansion coefficients for the ground and first and second excited states of the F, $F_H(OH^-)$ and $F_{H2}(OH^-)$ centers in CsCl.

State	F center	$F_H(OH^-)$ center	$F_{H2}(OH^-)$ center
Ground	$\|S\rangle$	$\|1A_1\rangle = 0.796\|S\rangle + 0.605\|S\rangle$	$\|1A_{1g}\rangle = \|S\rangle$
First excited	$\|X\rangle, \|Y\rangle, \|Z\rangle$	$\|2A_1\rangle = 0.605\|S\rangle - 0.796\|Z\rangle$	$\|2A_{2u}\rangle = \|Z\rangle$
Second excited		$\|2E\rangle = \|X\rangle, \|Y\rangle$	$\|2E_u\rangle = \|X\rangle, \|Y\rangle$

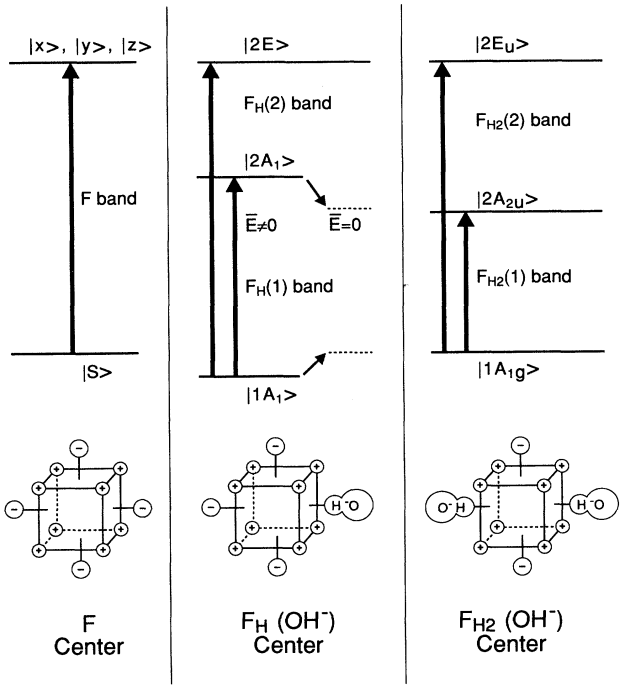

FIG. 3. Progression of the F band in CsCl due to perturbation by OH^- ions. The relative positions of energy levels are altered for purposes of illustration. The F band is split by the introduction of one OH^- ion, and the symmetry is reduced to C_{4v}. The $F_H(1)$ band is due to the $|1A_1\rangle \rightarrow |2A_1\rangle$ transition, where both energy levels are pushed apart by the OH^- ion's electric field; the dotted lines show the energy levels in the absence of an electric-field mixing. The second OH^- ion reduces the symmetry to D_{4h} and it cancels the electric field in the vacancy. With no electric-field mixing, the energy levels move closer together and produce the lower-energy $F_{H2}(1)$ band.

dient contributions to the energy eigenvalues. Comparison with the variational parameter values is presented in Table III, and it indicates the greater the potential and gradient contribution, the more localized the state: The ground state and excited state $|2A_{2u}\rangle$ are localized within the vacancy, whereas the $|2E_u\rangle$ state is more diffuse.

TABLE VI. Net OH^- dipole potential and electric-field gradient contributions to the energy eigenvalues of each state. All energies are in eV.

State	$\langle(V_{\alpha 0}+V_{\beta 0})\rangle$	$\langle(V_{\alpha 2}+V_{\beta 2})\rangle$
$\|1A_{1g}\rangle$	−0.75	−0−
$\|2A_{2u}\rangle$	−0.54	−0.31
$\|2E_u\rangle$	−0.06	−0.14

The second effect of the opposing dipoles is to cancel the electric field in the vacancy; therefore, the $|S\rangle$ and $|Z\rangle$ basis states of the $F_H(OH^-)$ center are no longer mixed together. It is worth noting that the vacancy electric field from each OH^- ion is quite small because the displacement and permanent dipoles are of about equal magnitudes and opposite in direction with a resultant dipole moment of 0.10×10^{-18} esu cm. The absence of the field in the vacancy eliminates the effective repulsion of the two levels, and as a result, the energy difference between them decreases: the ground-state ($|1A_1\rangle$) energy increases and the first-excited-state ($|2A_1\rangle$) energy decreases. Consequently, the new absorption band $F_{H2}(1)$ has a energy smaller than the $F_H(1)$ band.

Figure 3 illustrates the F-band evolution discussion above. It displays the progression from the F band to the two $F_H(OH^-)$ bands and then to the $F_{H2}(OH^-)$ bands, as brought about by the perturbation of the OH^- ions.

In summary, to the extent that the $F_H(OH^-)$ model calculation is valid, the $F_{H2}(OH^-)$-band separation is larger than that of the $F_H(OH^-)$ band because of the decoupling of electric-field-induced repulsion between the $|S\rangle$ and $|Z\rangle$ states produced by the additional OH^- ion.

ACKNOWLEDGMENTS

The author thanks Professor F. Lüty for sending results of numerous papers,[1,5–7,10] prior to publication, for several stimulating and informative discussions, and for a copy of Dr. Matthis Krantz's Ph.D. thesis.[34]

[1]Y. Yang and F. Lüty, Phys. Rev. Lett. **51**, 419 (1983).
[2]L. Gomes and F. Lüty, Phys. Rev. B **30**, 7194 (1984).
[3]P. W. Gash, Phys. Rev. B **34**, 5691 (1986).
[4]P. W. Gash, Phys. Rev. B **35**, 774 (1987).
[5]G. Halama, K. T. Tsen, S. H. Lin, F. Lüty, and J. B. Page, Phys. Rev. B **39**, 13 457 (1989).
[6]M. Krantz and F. Lüty, Phys. Rev. B **37**, 8412 (1988).
[7]V. Dierolf, H. J. Paus, and F. Lüty, Phys. Rev. B **43**, 9888 (1991).
[8]N. Nishimaki, Y. Matsusaka, and Y. Doi, J. Phys. Sci. Jpn. **33**, 424 (1971).
[9]W. B. Fowler, *Physics of Color Centers* (Academic, New York, 1968), Chap. 2.
[10]M. Krantz, F. Lüty, V. Dierolf, and H. J. Paus, Phys. Rev. B **43**, 9879 (1991).
[11]R. H. Bartram, A. M. Stoneham, and P. Gash, Phys. Rev. **176**, 1014 (1968).
[12]I. E. Cade, J. Chem. Phys. **47**, 2390 (1967).
[13]R. LeSar and R. G. Gordon, Phys. Rev. B **25**, 7221 (1982).
[14]R. D. Kirby, A. E. Hughes, and A. J. Sievers, Phys. Rev. B **2**, 481 (1970).
[15]I. Shepard and G. Feher, Phys. Rev. Lett. **15**, 194 (1965).
[16]U. Kuhn and F. Lüty, Solid State Commun. **2**, 281 (1964).
[17]H. Shore and L. Sander, Phys. Rev. B **6**, 1551 (1972).
[18]H. Werner, P. Rosmus, and E. Reinsch, J. Chem. Phys. **79**, 905 (1983).
[19]E. Clementi, IBM J. Res. Dev. (Suppl.) **9**, 2 (1965).
[20]F. Herman and S. Skillman, *Atomic Structure Calculations* (Prentice-Hall, Englewood Cliffs, NJ, 1965).
[21]G. K. Pandey and D. K. Skukla, Phys. Rev. B **3**, 4391 (1971).
[22]A. M. Stoneham, *Theory of Defects in Solids* (Oxford University Press, Oxford, 1975), p. 11.

[23]John L. Prather, *Atomic Energy Levels in Crystals,* Natl. Bur. Stand. (U.S.) Monograph 19 (U.S. GPO, Washington, D.C., 1961), p. 10.
[24]B. S. Gourary and F. J. Adrian, Phys. Rev. **105**, 1180 (1957).
[25]J. R. Tessman, A. H. Kahn, and W. Shockley, Phys. Rev. **92**, 890 (1953).
[26]Linus Pauling, *The Nature of the Chemical Bond,* 3rd ed. (Cornell University Press, Ithaca, 1960), p. 525.
[27]W. B. Fowler, *Physics of Color Centers* (Academic, New York, 1968), p. 60.
[28]P. Gash, Ph.D. thesis, University of Connecticut, 1970.
[29]R. C. Alig, Phys. Rev. B **2**, 2108 (1970).
[30]W. Weber and B. G. Dick, Phys. Status Solidi **36**, 723 (1969).
[31]W. E. Milne, *Numerical Calculus* (Princeton University Press, Princeton, NJ, 1949), p. 123.
[32]A. J. Freeman and P.-O. Löwden, Phys. Rev. **111**, 1212 (1958).
[33]W. E. Milne, *Numerical Calculus* (Ref. 31), p. 97.
[34]M. Krantz, Ph.D. thesis, Univeristy of Utah, 1987; p. 137.
[35]A. M. Stoneham, *Theory of Defects in Solids* (Ref. 22), p. 37.
[36]John R. Hardy and Arnold M. Karo, *The Lattice Dynamics and Statics of Alkali Halide Crystals,* (Plenum, New York, 1979), p. 198.
[37]M. Krantz, Ph.D. thesis, University of Utah, 1987, pp. 84 and 137.